Version auteur du papier de conférence : Cloëz Liam, Fontaine Michaël, Gilbin Alexandre and Barrière Thierry, Machinabilty of PLA obtained by injection molding under a dry milling process, 27th international Conference on Material Forming (ESAFORM 2024), Toulouse, France, april 2024

Machinability of PLA obtained by injection molding under a dry milling process

Liam Cloëz[1,2,a], Michaël Fontaine[1,b], Alexandre Gilbin[1,c] and Thierry Barrière[2,d]

[1] SUPMICROTECH, CNRS, institut FEMTO-ST, F-25000 Besançon, France
[2] Université de Franche-Comté, CNRS, institut FEMTO-ST, F-25000 Besançon, France

[a]liam.cloez@femto-st.fr, [b]michael.fontaine@ens2m.fr, [c]alexandre.gilbin@ens2m.fr, [d]thierry.barriere@univ-fcomte.fr

Keywords: Poly Lactic Acid , Injection Molding, Machining, Dry milling

Abstract

This paper is part of a study focusing on the elaboration of accurate component with complex geometries using bio-sourced as an alternative to petrochemical polymer. The bio-sourced and biodegradable in this study is composed of a Poly Lactic Acid (PLA) matrix and hemp fibers. The final component is obtained by injection followed by a machining operation. the final component is obtained by injection followed by a machining finishing operation. Injection molding will be carried out to be compared with 3D printing on economic, environmental, production and workpiece quality criteria. This paper focuses only on the combination of two processes, injection molding followed by machining on poly (L-lactic acid) or PLLA which is biobased and biodegradable. After injecting the workpiece, thermo-physical characterization tests are realized on PLLA polymer. Rheology, thermal and mechanical tests are carried out in order to study thermomechanical behavior and to understand material flow phenomena at different temperatures and shear rates. The objective of this paper is to overcome the technical challenges of milling this material without any lubricant. In an upcoming project, various machining operations will be carried out such as turning to study continuous cutting, or milling to study discontinuous cutting on workpieces reinforced with bio-sourced fibers as hemp.

Introduction

Over the decades, the growing use of polymer materials has changed our everyday lives, and they are now omnipresent, such as in medicine [1] or in civil construction [2]. However, this widespread popularity of polymers has often come at the expense of careful consideration of their ecological impact. While the versatility and durability of these materials make them ideal candidates for a variety of applications, it is becoming imperative to question our indiscriminate use of polymers.
This exploration raises essential questions about the need to modify our approach to more ecofriendly materials, at a time when ecological concerns are taking center stage in our collective consciousness. It is in this context that biosourced polymer materials, derived from renewable sources such as corn, sugarcane or algae, are emerging as promising solutions [3].
These polymers, often referred to as "bioplastics", offer the possibility of reducing dependence on non-renewable petrochemical resources, while limiting the greenhouse gas emissions associated with their production. Belboom *et al.* [4] shows that by carefully selecting the location and type of crops for the production of bio-based polymers, greenhouse gas emissions could be reduced for equivalent volumes of similar polymers derived from petrochemicals.

Some have focused on recyclability of these materials and their performance throughout their various life cycles as Schäfer *et al.* [5].
Injection molding is now a well-known and mature process to realize complex components in large scale and the machining of polymers has been studied, in turning or drilling processes. Milling of polymer parts is less investigated, especially for PLA. Rawal *et al.* [6] presents the various factors influencing the cutting of these materials, such as cutting parameters, cutting tool, polymer type, manufacturing method, and composite polymer properties. This is the reason why a characterization study on this material is necessary to analyze its thermal, mechanical and rheological behaviors before machining the injected parts. The correct parameters for molding components through injection will be selected based on results of the thermal and rheological study.

Materials and methods

Material
The material selected in this study is poly (L-lactic acid) or PLLA with D-lactide content of 0.5%, a density of 1.25 g.cm^{-3}, a melting temperature (T_m) between 170 °C and 180 °C and a glass transition temperature (T_g) of 58°C. It is provided by NaturePlast by the name PLI005 in pellet form. They recommend drying the material at 60 °C for 3 hours before any manufacturing process. However, according to a parametric study performed in our laboratory, the ideal drying parameters for PLI005 are 80 °C for a minimum of 5 hours, to minimize degradation caused by humidity during processing.

Differential Scanning Calorimetry (DSC)
Tests were carried out on SETARAM DSC131EVO to study the thermal behavior of the material. Only temperatures of transition phases such as melting (T_m), crystallization (T_c) and glass transition (T_g) were recorded. Pellets (for a mass of 25.4 g) taken from the PLA feedstock were placed into an aluminum crucible with a heating rate of 1 °C.min^{-1} from 25 °C to 195 °C and then was cooled with air to 25 °C.

Cone-and-plate rheometer
Two different rheometers were employed to analyze the rheological behavior of the material. The first rheometer HAAKE MARS is a cone-and-plate system, enabling the examination of the polymer's shear viscosity across shear rates ranging from 10^{-5} s^{-1} to 10^{2} s^{-1} at different temperatures. The sample is placed on the 35 mm diameter plate and the cone positioned above with an air gap angle (β) of 2 ° will rotate at a certain angular viscosity (ω) and then heated at the required temperature.

Capillary rheometer
The second rheometer is a capillary rheometer ROSAND RH2000. The polymer flows through a shear die with a diameter of 1 mm and a length of 16 mm. Pressures at the entrance and exit of the die are measured to determine the shear viscosity values. This system enables the measurement of polymer viscosity at higher shear rates ranging from 10^{2} s^{-1} to 10^{4} s^{-1}.

Tensile test
Tensile strength, elongation at break and Young's modulus were measured on injected-molded PLA specimens following the ISO 527-2 standard (Figure 1). Before the tensile test, specimens

were stored in a climatic chamber at 23 °C and 50% RH (relative humidity) for 7 days. The tensile testing press performed the C45 model from MTS. Tests were conducted with a crosshead speed of 2 mm.min^{-1} and a load cell of 12 kN.

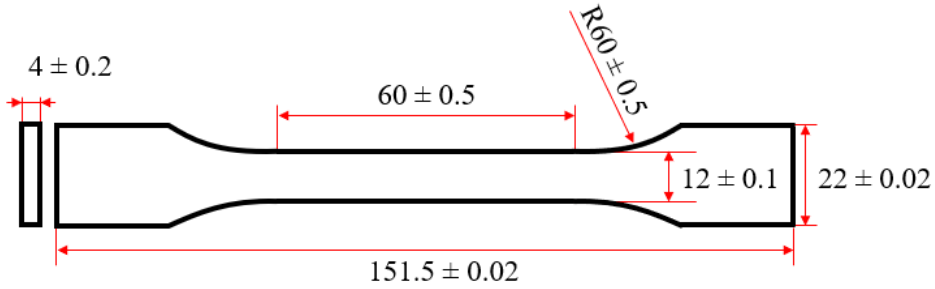

Figure 1 : Dimensions (mm) of tensile test specimens (ISO 527-2)

Injection molding

Table 1 : Injection molding parameters

Material	Feed zone [°C]	Transition zone [°C]	Transition zone [°C]	Metering zone [°C]	Mold temperature [°C]	Injection flow [g.s^{-1}]	Injection pressure [MPa]	Cooling time [s]
PLA	195	190	190	190	45	41	14	25

The injection molding was carried out using a BOY 22M with a clamping force of 220 kN. The materials were introduced into the injection molding press (Figure 2) in pellet form and injected to tensile test specimen with dimensions detailed in Figure 1 or milling block (Figure 3.C). The injection molding parameters are outlined in Table 1.

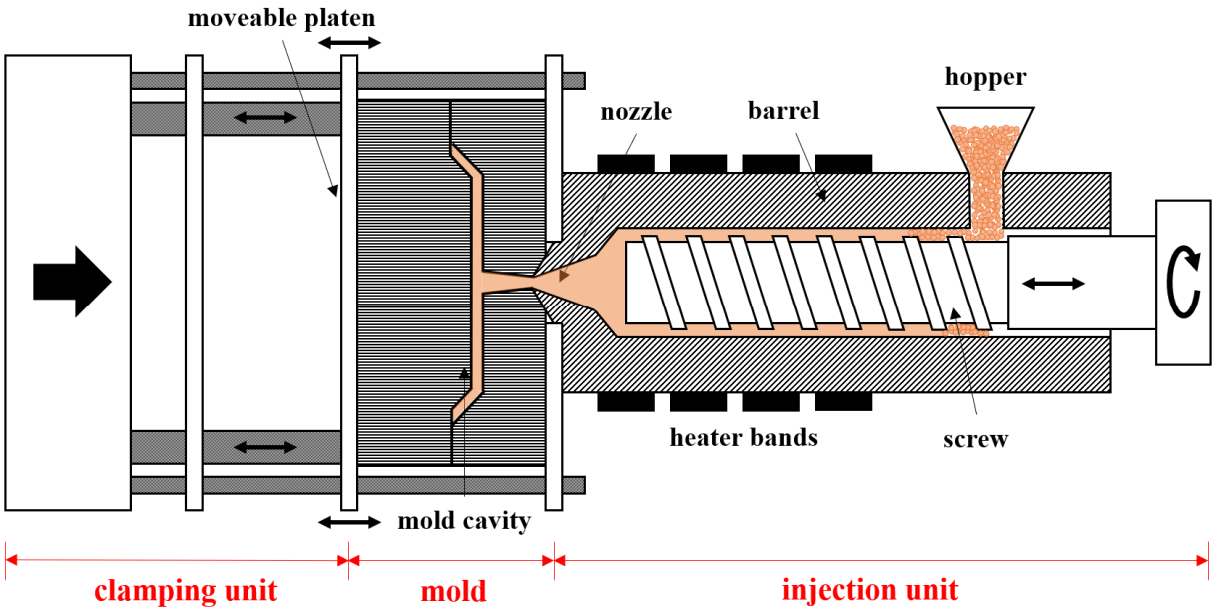

Figure 2 : Injection molding process

Machining

Dry machining tests were conducted on a DECKEL MAHO DMU35M milling machine. The specimen dimensions are detailed in Figure 3. In order to overcome technical challenges related to the machinability of PLA in dry conditions, slotting was chosen as initial machining operation. To optimize samples, six slots were made per piece (Figure 3). The cutting tool used for slotting was a 2-tooth end mill with a diameter of 6 mm, referenced as ELCO K0750.060. To measure cutting forces, PLA blocks were clamped onto the KISTLER 9129AA force sensor. For each measurement acquisition, the sampling frequency was set at 50 points per tooth pass, ranging from a minimum frequency of 1768 Hz to a maximum frequency of 8842 Hz.

Optical 3D measuring instrument / digital microscope

The microscope ALICONA InfiniteFocus was used to measure the surface roughness of the machined parts. Measurements (9 × 3 mm) were taken at the center of the groove in the longitudinal direction relative to the feed direction. Then the data analysis was processed using Digital Surf's MountainsMap software. Evaluation lengths and cut-off were chosen according to the ISO 21920 standard. Values of these two parameters vary depending on the measurement.

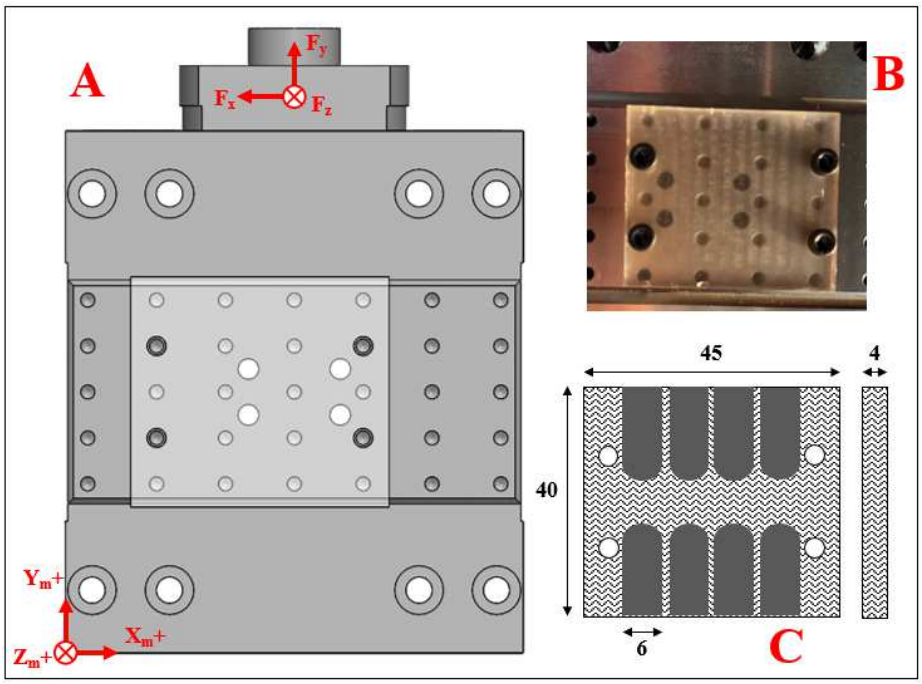

Figure 3 : CAD diagram of a PLA milling block fixed on the KISTLER sensor (A), photograph of the PLA block on the cutting forces sensor (B), geometry of a block after machining with 8 slots (C)

Results and discussion

Thermal properties

On the figure 4, the DSC thermogram is observed, showing various temperature peaks representing phase transitions of PLA. The first endothermic phase transition corresponds to the material's glass transition at a temperature (T_g) of 58 ± 1 °C. Then, the second phase transition is exothermic and corresponds to the crystallization of the material at a temperature (T_c) of 107 ± 1 °C and finally, a last endothermic phase transition is observable at a temperature (T_m) of 176 ± 1 °C. Temperature

values for the various phase transitions of our PLA are consistent with those provided by NaturePlast. The values may vary depending on the isomeric composition of PLA, but similar values are found as reported by Kasmi *et al.* [7], who also employed a semi-crystalline PLA.

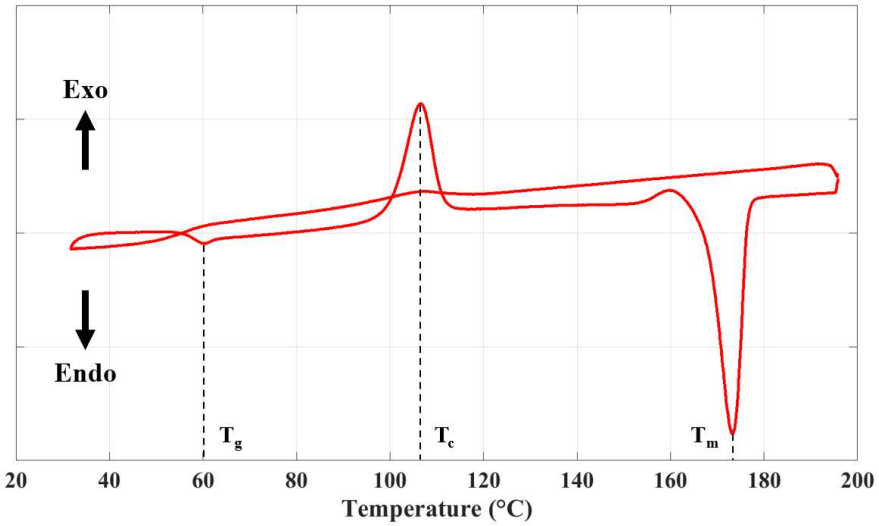

Figure 4 : DSC thermogram of PLA

Rheological properties

In Figure 5, a Newtonian plateau is observed at low shear rates (up to 1 s^{-1}). Subsequently, the shear viscosity decreases with increasing of the shear rate, showing a pseudoplastic behavior of PLA. Moreover, the shear viscosity decreases with the rising temperature, indicating a thermo-dependent response. These trend curves are similar to other rheological studies on PLA. Lacambra-Andreu *et al.* observes the same behaviors [8] but with higher values. Indeed, they studied an amorphous PLA with a different isomer composition, altering the physico-chemical parameters of the material and consequently the rheological behavior.

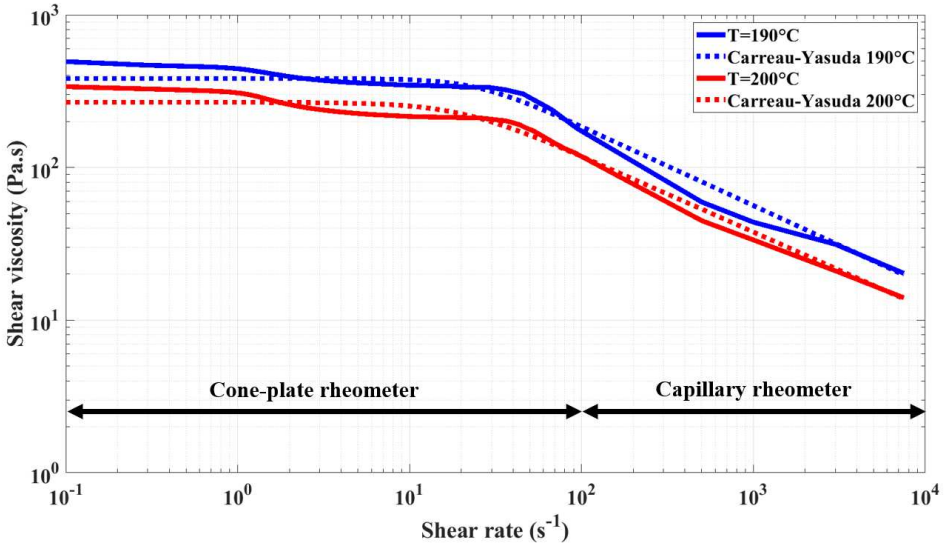

Figure 5 : Shear viscosity depending on shear rate for tested PLA at 190°C and 200°C and associated theoretical curves (eq.1)

The displayed temperatures were chosen based on the manufacturing process used. Indeed, as indicated in Table 1, the injection temperatures range from 190 °C to 200 °C.
Curves has been plotted according to the Carreau-Yasuda model (Eq. 1) to theoretically describe the rheological behavior based on the shear rate and model parameters (η_∞, η_0, λ, n, a). Model parameters has been fitted [9] based on the work of Ou :

$$\eta = \eta_\infty + (\eta_0 - \eta_\infty)(1 + (\lambda\dot{\gamma})^a)^{\frac{n-1}{a}} \quad (1)$$

$\dot{\gamma}$ is the shear rate and at 190 °C, a=2, n=0.48, η_∞=0 Pa.s, η_0=383.45 Pa.s, λ=0.04 s. The shear rate in 3D printing at the nozzle at this temperature is about 600 s^{-1} [8], and thus the shear viscosity would be approximately 80 Pa.s. For injection molding, the shear rate exceeds 1000 s^{-1}, and therefore, the shear viscosity would be less than 30 Pa.s.

Mechanical properties
The figure 6 illustrates the mechanical properties of the injected PLA using parameters stated in Table 1. In order to measure the longitudinal deformation, an MTS axial extensometer was attached to the effective section of the specimen. This curve indicates a brittle polymer by breaking without showing necking. The average values across several injected specimens for mechanical properties are as follows: elongation at break of 1.74 ± 0.19%, Young modulus of 2.91 ± 0.15 GPa and ultimate stress of 46 ± 2 MPa.

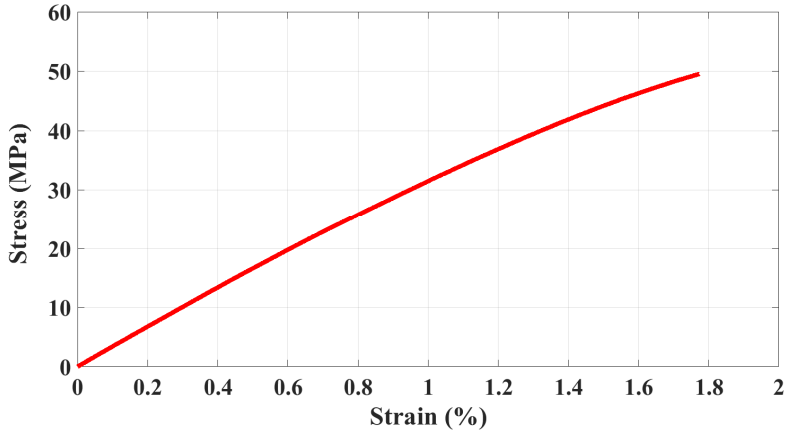

Figure 6 : Tensile curve of injected specimen of PLA

These values diverge from those available in the literature; indeed, Lay *et al.* or Lacambra-Andreu *et al.* presents the same ultimate stress [4,6], but the tensile modulus is divided by two and the elongation at break is multiplied by three compared to values in this study. Once again, the properties of PLA can vary from one grade to another. Thus, the studied PLA is more brittle than those presented by these authors. An explanation could be that differences arise from the prior conditioning cycle of the specimens.

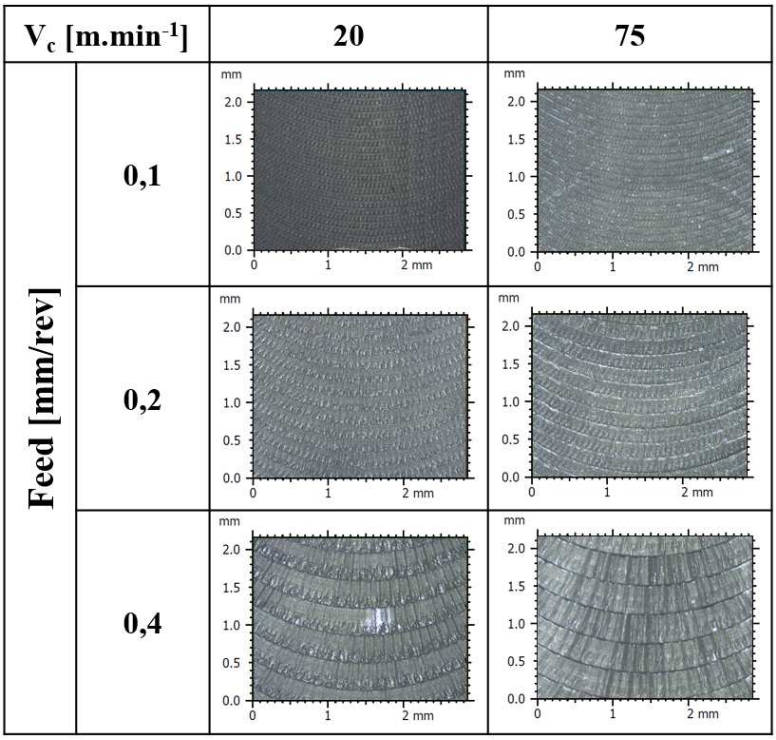

Figure 7 : Images of the six first slots captured by the microscope InfiniteFocus depending on the cutting parameters (for a_p = 2 mm)

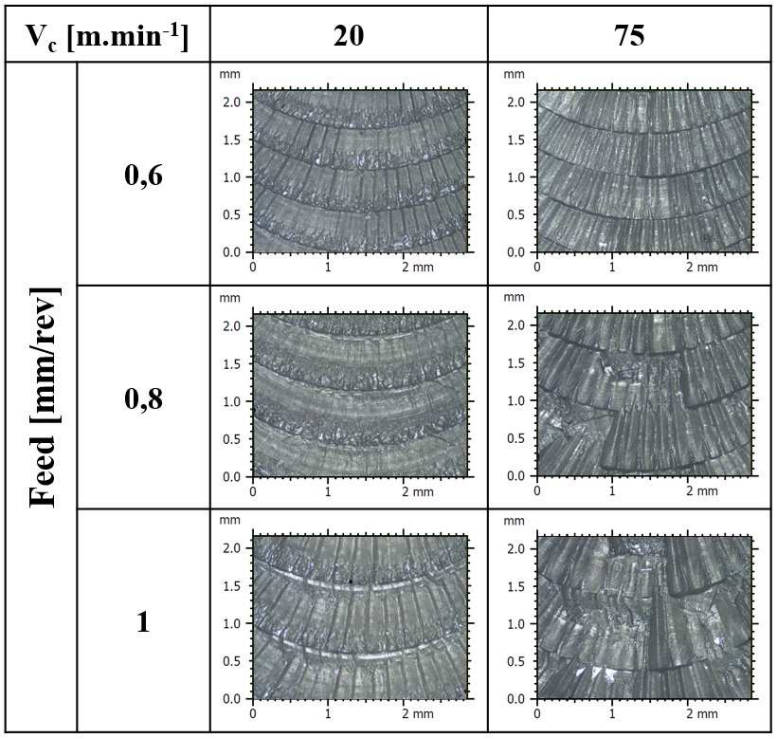

Figure 8 : Images of the six following slots captured by the microscope InfiniteFocus depending on the cutting parameters (for a_p= 2 mm)

Forces

For each of the machining tests conducted, the chip was discontinuous. In order to overcome technical barriers regarding PLA machining in dry conditions, tests were performed according to the NF E66-520 standard to study the tool-workpiece combination. Various tests were implemented to determine the cutting parameters (V_c, f_z, a_p and a_e). Tests at cutting speeds of 30, 40 and 50 m.min^{-1} were repeated three times. As for the other tests, they were not replicated and would therefore need to be reproduced to validate results. The specific cutting coefficient is calculated (Eq. 2) for the position of the cutting tool where material removal is equal to the feed per tooth. Thus, it is assumed that the cutting force is the maximal force along the X-axis, considering that F_y is significantly lower than F_x. These forces are averaged peak-to-peak with a measurement uncertainty around 5%. This assumption remains acceptable given that this is a comparative study between cutting parameters. The curve in Figure 9.A represents the average specific cutting coefficient (K_c) as function of the cutting speed (V_c). The specific cutting coefficient can be determined by the equation 2, where F_c is the cutting force.

$$K_c = \frac{F_c}{f_z \cdot a_p} \quad (2)$$

Limited by the machine used, the maximum cutting speed applied is here of 100 m.min^{-1}. It can be concluded based on the standard that the minimum cutting speed in our configuration lies between 50 m.min^{-1} and 60 m.min^{-1} by limiting variation. Similarly, the feed per tooth is determined by the specific cutting coefficient (Figure 9.B). Thus, it can be concluded that the minimum feed rate is 0.4 mm/rev, and the maximum is 0.8 mm/rev, with the occurrence of catastrophic phenomena on the slot edge, such as large material removal. Next, a test campaign was conducted for the depth of cutting with no significant change in the cutting coefficient, ranging from 0.25 mm to 3 mm, limited by the geometric dimensions of the workpiece.

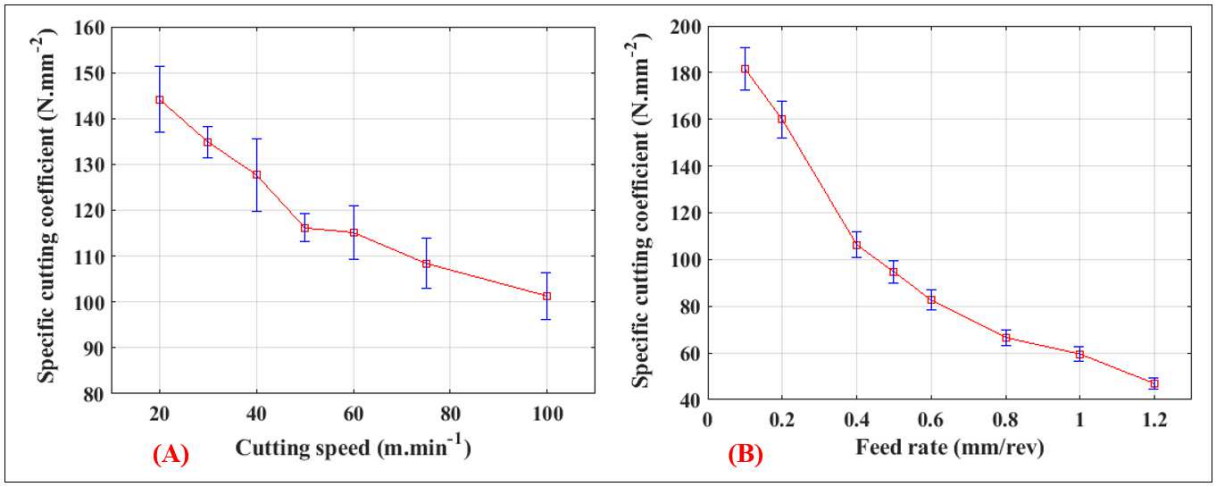

Figure 9 : Effect of cutting speed (a_p = 2 mm, f = 0.4 mm/rev) on the average specific cutting coefficient (K_c) in dry milling of PLA (A). Effect of feed rate (a_p = 2 mm, V_c = 75 m.min^{-1}) on the average specific cutting coefficient (K_c) in dry milling of PLA (B).

Surface roughness

A study was conducted to compare surface roughness within the slots for different cutting speeds and feed per tooth for a depth of cut of 2 mm. The various captures taken by the digital microscope are shown in figure 7 and figure 8 as a function of these cutting parameters. Figure 10 shows the average surface roughness on both surface and linear parameters as a function of cutting speed and feed per revolution. Similar trends are observed between the two roughness measures. Beyond a feed of 0.4 mm/rev, an increase in roughness is observed at various cutting speeds. An increase in cutting speed can lead to partial melting or local deformation of the polymer, resulting in a rougher surface. Surface roughness increases linearly with feed, which is less the case for linear roughness. Indeed, Ra values remain constant from a feed of 0.5 mm/rev up to 1 mm/rev. These curves highlight limitations of linear criteria for milled surfaces.

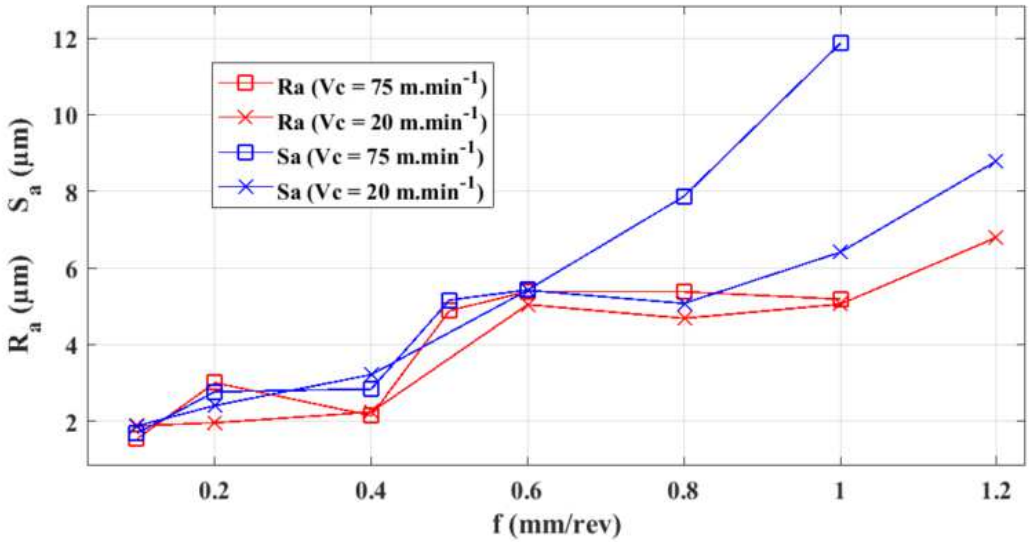

Figure 10 : Effect of cutting speed and feed per tooth on the surface roughness (a_p = 2 mm)

Conclusions and prospects

This paper presents preliminary results on PLA machining in dry conditions, and allow us to select injection molding (Table 1) and cutting parameters (a minimum cutting speed of 60 m.min^{-1}, and a feed per revolution between 0.2 and 0.4 mm/rev) potentially suitable for this material, especially when it will be reinforced with bio-sourced fibers such as hemp. For the dry machining of the polymer, it is about finding a compromise in cutting parameters between surface quality and cutting quality. At a cutting speed of 20 m.min^{-1}, the surface roughness of the slot is approximately 6.5 µm, and the cutting force is 58 N. For a test with a higher cutting speed (75 m.min^{-1}), the surface roughness is multiplied by 2 (~ 12 µm), and the cutting force decreases slightly (~ 43 N). It is necessary to avoid agglomeration of molten chips on the tool, burrs, and surface degradation. Thus, additional tests will be conducted to find this balance point for dry milling, by studying burrs and thermal aspects for values of cutting parameters that will be extended. Further studies are underway on the same process sequence, considering different factors for the machining of these materials such as the process (turning, milling, drilling), the lubricant (air flow, water) or the cutting tool. The final purpose is also to compare machinability of reinforced PLA pre-formed by injection molding and 3D printing (Pellet Additive Manufacturing). Several studies will be necessary to achieve machining of the printed polymer composite. Once these samples have been obtained, the same type of machining tests will be carried out.

Acknowledgments

This work was carried out within the Manufacturing 21 working group, which gathers about 20 French research laboratories. The covered topics are manufacturing processes optimization, tool-workpiece interaction, and emerging manufacturing methods. The authors would like to thank the French Ministry of Higher Education and Research for funding the thesis grant, and the MIFHYSTO and AMETISTE platforms of the Applied Mechanics Department of the FEMTO-ST Institute for access to experimental facilities.

References

[1] S. Ramakrishna, J. Mayer, E. Wintermantel, and K. W. Leong, "Biomedical applications of polymer-composite materials: a review," *Compos. Sci. Technol.*, vol. 61, no. 9, pp. 1189–1224, Jul. 2001, doi: 10.1016/S0266-3538(00)00241-4.

[2] S. S. Pendhari, T. Kant, and Y. M. Desai, "Application of polymer composites in civil construction: A general review," *Compos. Struct.*, vol. 84, no. 2, pp. 114–124, Jul. 2008, doi: 10.1016/j.compstruct.2007.06.007.

[3] I. Vroman and L. Tighzert, "Biodegradable Polymers," *Materials*, vol. 2, no. 2, pp. 307–344, Apr. 2009, doi: 10.3390/ma2020307.

[4] S. Belboom and A. Léonard, "Does biobased polymer achieve better environmental impacts than fossil polymer? Comparison of fossil HDPE and biobased HDPE produced from sugar beet and wheat," *Biomass Bioenergy*, vol. 85, pp. 159–167, Feb. 2016, doi: 10.1016/j.biombioe.2015.12.014.

[5] H. Schäfer, C. Pretschuh, and O. Brüggemann, "Reduction of cycle times in injection molding of PLA through bio-based nucleating agents," *Eur. Polym. J.*, vol. 115, pp. 6–11, Jun. 2019, doi: 10.1016/j.eurpolymj.2019.03.011.

[6] S. Rawal, A. M. Sidpara, and J. Paul, "A review on micro machining of polymer composites," *J. Manuf. Process.*, vol. 77, pp. 87–113, May 2022, doi: 10.1016/j.jmapro.2022.03.014.

[7] S. Kasmi, J. Cayuela, B. D. Backer, E. Labbé, and S. Alix, "Modified Polylactic Acid with Improved Impact Resistance in the Presence of a Thermoplastic Elastomer and the Influence of Fused Filament Fabrication on Its Physical Properties," *J. Compos. Sci.*, vol. 5, no. 9, p. 232, Sep. 2021, doi: 10.3390/jcs5090232.

[8] X. Lacambra-Andreu, X. P. Morelle, A. Maazouz, J.-M. Chenal, and K. Lamnawar, "Rheological investigation and modeling of healing properties during extrusion-based 3D printing of poly(lactic-acid)," *Rheol. Acta*, vol. 62, no. 1, pp. 31–44, Jan. 2023, doi: 10.1007/s00397-022-01377-6.

[9] H. Ou, "Modélisation multi-physiques et simulations numériques du moulage par injection mono et bi-matières thermoplastique / silicone liquide," Matériaux, Université de Franche-Comté, 2015.

[10] M. Lay, N. L. N. Thajudin, Z. A. A. Hamid, A. Rusli, M. K. Abdullah, and R. K. Shuib, "Comparison of physical and mechanical properties of PLA, ABS and nylon 6 fabricated using fused deposition modeling and injection molding," *Compos. Part B Eng.*, vol. 176, p. 107341, Nov. 2019, doi: 10.1016/j.compositesb.2019.107341.